Earth and Planetary Science Letters 440 (2016) 20–32

Contents lists available at ScienceDirect

Earth and Planetary Science Letters

www.elsevier.com/locate/epsl

Bunbury Basalt: Gondwana breakup products or earliest vestiges of the Kerguelen mantle plume?

Hugo K.H. Olierook [a,b,*], Fred Jourdan [a,c], Renaud E. Merle [a,d], Nicholas E. Timms [a], Nick Kusznir [b], Janet R. Muhling [a,e]

[a] Department of Applied Geology, Curtin University, GPO Box U1987, Perth, WA 6845, Australia
[b] Department of Earth, Ocean and Ecological Sciences, University of Liverpool, 4 Brownlow Street, Liverpool, L69 3GP, UK
[c] Western Australian Argon Isotope Facility & John de Laeter Centre, Curtin University, GPO Box U1987, Perth, WA 6845, Australia
[d] Research School of Earth Sciences, Australian National University, 142 Mills Road, Acton, ACT 0200, Australia
[e] Centre for Microscopy, Characterisation and Analysis, University of Western Australia, Crawley, Perth, WA 6009, Australia

ARTICLE INFO

Article history:
Received 20 October 2015
Received in revised form 2 February 2016
Accepted 2 February 2016
Available online 15 February 2016
Editor: A. Yin

Keywords:
large igneous provinces
Perth Basin
continental flood basalts
crustal basement thickness
western Australian margin
$^{40}Ar/^{39}Ar$ geochronology

ABSTRACT

In this contribution, we investigate the role of a mantle plume in the genesis of the Bunbury Basalt using high-precision $^{40}Ar/^{39}Ar$ geochronology and whole-rock geochemistry, and by using crustal basement thickness of the eastern Indian Ocean and the western Australian continent. The Bunbury Basalt is a series of lava flows and deep intrusive rocks in southwestern Australia thought to be the earliest igneous products from the proto-Kerguelen mantle plume. Nine new plateau ages indicate that the Bunbury Basalt erupted in three distinct phases, at 136.96 ± 0.43 Ma, 132.71 ± 0.43 Ma and 130.45 ± 0.82 Ma. All Bunbury Basalt samples are enriched tholeiitic basalts with varying contributions from the continental lithosphere that are similar to other Kerguelen plume-products. Based on plate reconstructions and the present geochronological constraints, the eruption of the oldest Bunbury Basalt preceded the emplacement of the Kerguelen large igneous province by at least 10–20 m.y. Such age differences between a precursor and the main magmatic event are not uncommon but do require additional explanation. Low crustal stretching factors beneath the Bunbury Basalt ($\beta \approx 1.4$) indicate that decompression melting could not have been generated from asthenospheric mantle with a normal chemistry and geotherm. An elevated geotherm from the mantle plume coupled with the geochemical similarity between the Bunbury Basalt and other Kerguelen plume-products suggests a shared origin exists. However, new age constraints of the oldest Bunbury Basalt are synchronous with the breakup of eastern Gondwana and the initial opening of the Indian Ocean at *ca.* 137–136 Ma, which may mean an alternative explanation is possible. The enriched geochemistry can equally be explained by a patch of shallow mantle beneath the southern Perth Basin. The patch may have been enriched during Gondwana suturing at *ca.* 550–500 Ma, during early rifting events by magmatic underplating or by intruded melts into the subcontinental lithospheric mantle. This enriched geochemical signature would then be sufficient to trigger decompression melting from passive rifting between Greater India and Australia with no contribution from the Kerguelen hotspot. We conclude that although the proto-Kerguelen hotspot is certainly a possible explanation for the genesis of the Bunbury Basalt, decompression melting of an enriched patch of subcontinental lithospheric mantle is an alternative theory.

1. Introduction

The mechanisms and underlying causes of supercontinent breakup and their dispersal into smaller continental plates are still strongly debated (e.g., Whitmarsh et al., 2001). Possible causes include unusually hot mantle upwellings, known as deep-rooted mantle plumes, or changes in plate-boundary driving forces. One of the key manifestations of a plume-influenced breakup is thought to be the presence of continental flood basalts temporally associated with breakup, resulting in a volcanic passive margin (Franke, 2013). A plume origin for some continental flood basalt provinces has been vigorously challenged in the past two decades (e.g., Anderson, 1994; van Wijk et al., 2001). In contrast, passive margins formed solely by lithospheric stretching are magma-poor,

* Corresponding author at: Department of Earth, Ocean and Ecological Sciences, University of Liverpool, 4 Brownlow Street, Liverpool, L69 3GP, UK. Tel.: +44 7903116690.
E-mail address: h.olierook@liverpool.ac.uk (H.K.H. Olierook).

http://dx.doi.org/10.1016/j.epsl.2016.02.008

with very little associated volcanism (Franke, 2013). Volcanism potentially coeval with the breakup of Greater India and Australia–Antarctica occurs along the western Australian passive margin, but its volumes are transitional between these two endmembers. There are abundant volcanic products along the northern margin in the Houtman Sub-basin, the Wallaby Plateau and the Cuvier Margin (Borissova et al., 2015; Olierook et al., 2015a). Some 1000 km further south, the only known instance of breakup-related volcanism is the Bunbury Basalt located in the onshore Perth Basin.

The origin of the Bunbury Basalt has been attributed to melting as a result of the interaction between what has now manifested itself as the Kerguelen deep-rooted mantle plume (i.e., proto-Kerguelen plume) and the continental lithosphere (Frey et al., 1996; Ingle et al., 2004, 2002). Indeed, the Bunbury Basalt shares geochemical characteristics with the Kerguelen archipelago but also with several other occurrences attributed to the Kerguelen hotspot, such as the 117–118 Ma continental Rajmahal Traps in India and present-day Indian Ocean mid-ocean ridge basalts (MORBs) (Frey et al., 1996; Ingle et al., 2004, 2002). Nevertheless, this hypothesis is based on sparse geochronological data, and Kerguelen hotspot activity and the eruption of the Bunbury Basalt have never been confirmed to be coeval. The oldest eruption recorded on the Kerguelen Plateau is currently constrained by $^{40}Ar/^{39}Ar$ dating to *ca.* 119 Ma (Coffin et al., 2002; Duncan, 2002). If the Kerguelen Plateau is situated entirely on oceanic crust, except for the Elan Bank microcontinent (Borissova et al., 2003), the oldest possible age for the onset of magmatism is no older than the age of the oceanic floor estimated at *ca.* 128–126 Ma (Williams et al., 2011). However, if the southern and central part of the Kerguelen Plateau is underlain by remnants of stretched continental crust as suggested by Coffin et al. (2002) and Bénard et al. (2010), continental lava flows or intrusions could be present. In this case, magmatic occurrences could have been emplaced before continental rifting and before the isolation of this continental fragment. As a consequence, these magmas would be the oldest evidence of the Kerguelen Plateau magmatic activity and could be older than 128–126 Ma. However, there is no evidence of such magmas as yet. The flows of the Bunbury Basalt are currently believed to have erupted during two events at 123.4 ± 1.8 Ma (2σ) at Black Point (Cape Gosselin) and 132.2 ± 0.6 Ma (2σ) at Cape Casuarina (Coffin et al., 2002; Frey et al., 1996; Pringle et al., 1994). However, those ages are based on $^{40}Ar/^{39}Ar$ dating of whole rocks and one sample of plagioclase. $^{40}Ar/^{39}Ar$ analyses performed on whole-rock samples have been demonstrated to be unreliable due to the younging effect of alteration (Verati and Jourdan, 2014) and therefore the published ages should be reassessed using picked mineral grains and modern analytical instruments.

The Bunbury Basalt could also have been produced by the partial melting of shallow-level mantle material due to either heat provided by the proto-Kerguelen plume or by passive rise prior to continental breakup (decompression melting). However, the geochemical characteristics of the basalts cannot be explained solely by melt derived from depleted asthenosphere but also requires an enriched component. This enriched component could be derived from the Kerguelen hotspot or the subcontinental lithospheric mantle (SCLM; Ingle et al., 2004) and, therefore, the origin of the Bunbury Basalt remains uncertain. The mechanism by which the Bunbury Basalt magma was transported from its melt site to its eruptive center(s) also remains poorly constrained (Olierook et al., 2015b). The origin and magma transport mechanisms of the Bunbury Basalt are important for understanding the early sequence of volcanic events that occurred during continental breakup and formation of new oceanic crust. To gain this understanding, a precise and accurate chronology of events is necessary.

Here we investigate the chronology of the eruption of the Bunbury Basalt by $^{40}Ar/^{39}Ar$ geochronology on 10 plagioclase separates using an ARGUS VI multi-collector machine. We clarify the temporal relationships between the eruption of the basalts, the breakup of Greater India and Australia, the emplacement of the Kerguelen large igneous province and provide whole rock major and trace element compositions of the samples for a robust comparison with other volcanic rocks related to Kerguelen hotspot magmatism in the Indian Ocean. We have also estimated crustal basement thickness to facilitate assessment of the magma melt-to-eruption transport mechanisms. We integrate this information to ultimately ask the question: was a mantle plume responsible and necessary for the generation of the Bunbury Basalt or is there an alternative explanation for its genesis?

2. Geological background

Prior to its breakup, eastern Gondwana comprised present-day Australia, Antarctica, Greater India, Madagascar and several continental fragments that have since drifted to form the Indian Ocean. The timing of initial breakup of eastern Gondwana along the western Australian margin has been constrained to *ca.* 137–136 Ma using recent plate reconstructions and palynological biozones from underlying strata (Gibbons et al., 2012; Jones et al., 2012), although the oldest confirmed sea floor spreading anomaly in the Indian Ocean adjacent to Australia is chron M10 (ca. 134 Ma, Williams et al., 2013).

The Bunbury Basalt in southwestern Western Australia represents the earliest recorded volcanism potentially coeval with continental breakup of Greater India and Australia. The Bunbury Basalt is a series of lava flows (and possibly scarce sheeted intrusive rocks), situated largely within the north–south striking, fault-bound Bunbury Trough of the Perth Basin, and encroaching onto the Yilgarn Craton to the east and the Vasse Shelf to the west (Fig. 1, Olierook et al., 2015b). The southern Perth Basin contains up to 12 km of sedimentary fill, constrained from geophysical exploration and petroleum wells, ranging in age from the Permian to Recent (Olierook et al., 2015c). During the Early Cretaceous, the Bunbury Basalt lava flows erupted from vent sites postulated to lie at intersections of minor faults with the basin-bounding Darling Fault. They were extruded as three distinct flows into two deeply-incised paleovalleys that form the Valanginian breakup unconformity (Olierook et al., 2015b). The western paleovalley, the Bunbury Paleovalley, comprises both an upper and lower flow, with interflow siltstone and claystone that represents a volcanic hiatus of *ca.* 2.5 m.y. at *ca.* 136 Ma (Backhouse, 1988). The eastern paleovalley, the Donnybrook Paleovalley, hosts a continuous layer of basalt and is interpreted to be a single flow. The Donnybrook Paleovalley crosscuts the Bunbury Paleovalley and the former is therefore interpreted to be younger than the latter (Olierook et al., 2015b). Possibly comagmatic, deep-seated, discontinuous dolerite bodies intruded into Permian and Triassic sedimentary rocks at depths of 2700–4600 m below sea level. Since the formation of the breakup unconformity, the southern Perth Basin has accumulated relatively little preserved sedimentary fill due to rift-related and epeirogenic exhumation, so that the Bunbury Basalt is relatively accessible for sampling (Olierook and Timms, in press).

The Bunbury Basalt has been split into two geochemical groups based on their degree of continental contamination: Casuarina-type (*ca.* 132 Ma) and Gosselin-type (no reliable age data) (Coffin et al., 2002; Frey et al., 1996). The less-contaminated Casuarina group, assumed to most closely represent the original magmatic source, shows initial Sr–Nd–Pb–Hf–Os isotopic ratios similar to the continental Rajmahal Traps in India (Ingle et al., 2004, 2002). The latter have been dated by $^{40}Ar/^{39}Ar$ at *ca.* 118.1 ± 0.6 Ma based on a mini-plateau (including 62% of the ^{39}Ar released). Geochemical,

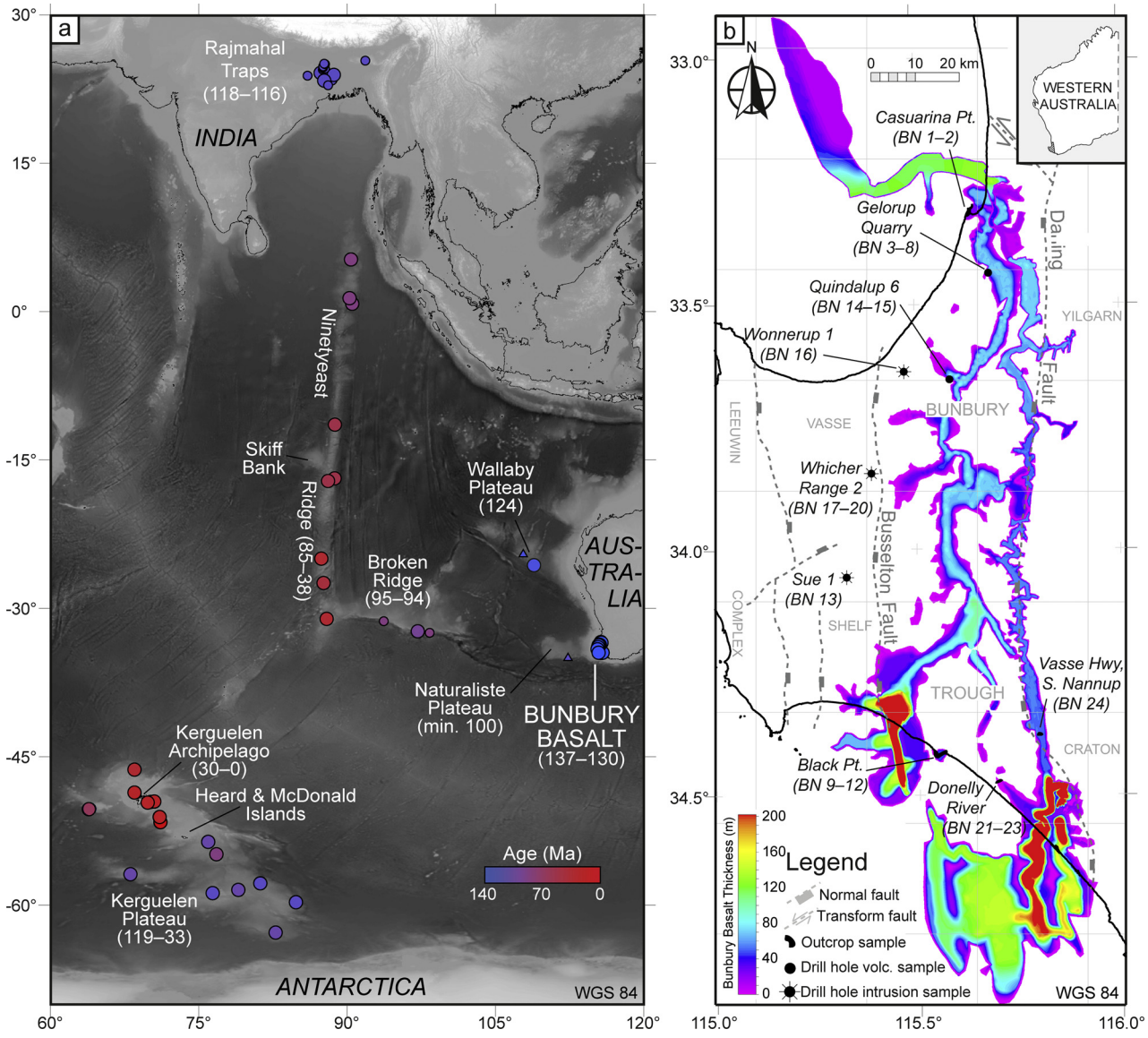

Fig. 1. (A) Bathymetric map of the Indian Ocean in the vicinity of the margin of Western Australia, after Amante and Eakins (2009). Major bathymetric features of the Indian Ocean and locations of dated extrusive rocks recovered from DSDP, ODP, IODP and industry volcanic basement sites are indicated after Coffin et al. (2002). Age data (in Ma) is indicated by colored circles, from various sources (Coffin et al., 2002; Olierook et al., 2015a; Pyle et al., 1995). Note that data from intrusive rocks (including lamprophyres) are not included on this map. (B) Map of onshore southwestern Australia showing the position and thickness of the Bunbury Basalt, modified from Olierook et al. (2015b). Sampled outcrops and drill holes are indicated.

temporal and geodynamic constraints indicate that the Rajmahal Traps are derived from the Kerguelen hotspot. The Bunbury Basalt also shares some of the chemical characteristics of present-day Indian Ocean MORBs (Klein et al., 1991). Aside from the Kerguelen Plateau, other Kerguelen-plume related oceanic flood basalts include Ninetyeast Ridge and Broken Ridge in the Indian Ocean (Coffin et al., 2002).

3. Sample descriptions

Twenty-four basalt samples were collected, including sixteen hand samples from outcrops and quarries, one interval of drill core, and ditch cuttings from two shallow water wells and five deep petroleum wells (Fig. 1b, Table 1). The Gelorup quarry samples were not collected *in situ*, but rather from blasted wall rock, and so stratigraphic relationships between samples are uncertain. Consultation with mine geologists has confirmed that two flows are present in the quarry, separated by a thin sedimentary layer. Flow differentiation for all other samples used the 3D model of the Bunbury Basalt are based on maps produced by Olierook et al. (2015b). Outcrop exposures, hand samples and thin sections indicate the Bunbury Basalt comprises dark grey, sparsely vesicular, porphyritic, fine-grained mafic rocks (Fig. 2). Casuarina-type localities (cf. Frey et al., 1996) include Casuarina Point, the upper flow in the Gelorup basalt quarry, Donnelly River and Quindalup 6, where samples are typically glomero- to microporphyritic with phenocrysts of plagioclase, and microphenocrysts of clinopyroxene and opaque oxides (Fig. 2b, f). Variably colored and altered glass is common in these samples. Gosselin-type localities (Frey et al., 1996) include Black Point, the lower flow of the Gelorup Quarry and the roadside south of Nannup, where samples are fine- to medium-grained and macroporphyritic with phenocrysts of plagioclase, clinopyroxene and opaque minerals and little to no glass (Fig. 2d). The deep intrusive rocks tend to have similar petrographic characteristics to Gosselin-type basalts, but are slightly coarser grained. Olivine is

Table 1
Location of newly-collected samples for the Bunbury Basalt lava flows and associated intrusive rocks. Flow context from Olierook et al. (2015b). Pv. = Paleovalley.

Sample no.	Coordinates[a]		Well/area name	Flow context	Depth (m)	
	Latitude	Longitude			Start	End
BN 1	−33.321	115.631	Casuarina Point	Bunbury Pv., upper flow	–	–
BN 2	−33.317	115.633	Casuarina Point	Bunbury Pv., upper flow	–	–
BN 3	−33.407	115.654	Gelorup Quarry	Bunbury Pv., upp./low. flow	–	–
BN 4	−33.407	115.654	Gelorup Quarry	Bunbury Pv., upp./low. flow	–	–
BN 5	−33.398	115.654	Gelorup Quarry	Bunbury Pv., upp./low. flow	–	–
BN 6	−33.398	115.654	Gelorup Quarry	Bunbury Pv., upp./low. flow	–	–
BN 7	−33.397	115.651	Gelorup Quarry	Bunbury Pv., upp./low. flow	–	–
BN 8	−33.397	115.651	Gelorup Quarry	Bunbury Pv., upp./low. flow	–	–
BN 9	−34.418	115.542	Black Point	Bunbury Pv., ? Flow	–	–
BN 10	−34.423	115.541	Black Point	Bunbury Pv., ? Flow	–	–
BN 11	−34.422	115.541	Black Point	Bunbury Pv., ? Flow	–	–
BN 12	−34.422	115.551	Black Point	Bunbury Pv., ? Flow	–	–
BN 13	−34.065	115.319	Sue 1	Deep-seated intrusives	2860.1	2860.4
BN 14	−33.641	115.586	Quindalup 6	Bunbury Pv., upper flow	42.0	51.0
BN 15	−33.641	115.586	Quindalup 6	Bunbury Pv., lower flow	63.0	72.0
BN 16	−33.631	115.473	Wonnerup 1	Deep-seated intrusives	3249.1	3261.4
BN 17	−33.841	115.384	Whicher Range 2	Deep-seated intrusives	2785.0	2805.0
BN 18	−33.841	115.384	Whicher Range 2	Deep-seated intrusives	3020.0	3040.0
BN 19	−33.841	115.384	Whicher Range 2	Deep-seated intrusives	3280.0	3300.0
BN 20	−33.841	115.384	Whicher Range 2	Deep-seated intrusives	3385.0	3405.0
BN 21	−34.483	115.685	Donnelly River	Donnybrook Pv.	–	–
BN 22	−34.481	115.689	Donnelly River	Donnybrook Pv.	–	–
BN 23	−34.480	115.694	Donnelly River	Donnybrook Pv.	–	–
BN 24	−34.378	115.793	Vasse Hwy, S. Nannup	Donnybrook Pv.	–	–

[a] All coordinates use GCS WGS84.

absent in all samples. All samples show amygdales and minor alteration of groundmass.

4. Analytical techniques

4.1. $^{40}Ar/^{39}Ar$ geochronology

Thirteen fresh samples were selected from the three lava flows and six intrusive rocks for $^{40}Ar/^{39}Ar$ dating. Samples were crushed and minerals were separated using a Frantz magnetic separator. The non-magnetic fraction was carefully hand-picked under a binocular microscope to select unaltered, optically transparent, 125–212 µm-size plagioclase grains. Plagioclase crystals from the Casuarina-type basalts were pristine, whereas grains from the Gosselin-type and the deep intrusive rocks were slightly altered. The selected plagioclase grains were leached in diluted (5 N) HF for one minute and then thoroughly rinsed with distilled water in an ultrasonic cleaner. Samples were loaded into several large wells of 1.9 cm diameter and 0.3 cm depth aluminum discs. The discs were Cd-shielded to minimize undesirable nuclear interference reactions and irradiated for 40 hours in the US Geological Survey nuclear reactor (Denver, USA) in central position over two irradiations.

The $^{40}Ar/^{39}Ar$ analyses were performed at the Western Australian Argon Isotope Facility at Curtin University. Three samples (BN 6, 10 & 12) were run on a MAP 215–50 mass spectrometer and yielded low age precision due to the unusually low K/Ca ratio of the plagioclase crystals (see supplementary material). Ten samples were run on a recently acquired ARGUS VI. These samples yielded much better age precision than those run on the MAP 215–50 due to better electronics and detectors resulting in better sensitivity, lower blanks and greater stability. Aliquots of BN 10 and 12 were also run on the ARGUS VI to assess how much more precise this new instrument was. The ages were calculated using Hb3gr hornblende and GA1550 biotite neutron flux monitors, for which ages of 1081 ± 1.189 Ma and 99.738 ± 0.100 Ma, respectively, were used (Jourdan et al., 2006; Renne et al., 2011, 1998). The mean J-values computed from standard grains on the ARGUS VI are $0.01127800 \pm 0.00001804$ (0.16%) and $0.00081110 \pm 0.00000057$ (0.07%), and $0.00848400 \pm 0.00001600$ (0.19%) for the MAP instrument, all determined as the average and standard deviation of J-values of the small wells for each irradiation disc. Mass discrimination was monitored using an automated air pipette and provided a mean value of 0.99386 ± 0.00050 per dalton on the ARGUS VI. The correction factors for interfering isotopes were $(^{39}Ar/^{37}Ar)_{Ca} = 7.30 \times 10^{-4}$ (±11%), $(^{36}Ar/^{37}Ar)_{Ca} = 2.82 \times 10^{-4}$ (±1%) and $(^{40}Ar/^{39}Ar)_{K} = 6.76 \times 10^{-4}$ (±32%).

Our criteria for the determination of plateaus are as follows: plateaus must include at least 70% of ^{39}Ar. The plateaus should be distributed over a minimum of 3 consecutive steps agreeing at 95% confidence level and satisfying a probability of fit (P) of at least 0.05. Plateau ages are given at the 2σ level and are calculated using the mean of all the plateau steps, each weighted by the inverse variance of their individual analytical error. All sources of uncertainties are included in the calculation.

4.2. Major and trace element geochemistry

Whole-rock major and trace element geochemistry data were acquired for all samples, with the exception of BN 20 due to the low volume of available material. Samples were crushed with a tungsten carbide mill and analyzed at Genalysis Laboratory Services, Perth. Major elements and Cr_2O_3 were fused with lithium borate and analyzed via Inductively Coupled Plasma Optical Emission Spectroscopy (ICP-OES). Trace elements were fused by lithium borate, except Ni, Co and Pb that were fused by acid digestion. Trace elements were analyzed via ICP Mass Spectrometry (ICP-MS).

4.3. Crustal basement thickness

Crustal basement thickness has been determined from gravity inversion using the method of Chappell and Kusznir (2008) and Alvey et al. (2008). The 3D spectral gravity inversion methodology incorporates a lithosphere thermal gravity anomaly correction and uses as input public domain satellite free-air gravity anomaly (Sandwell and Smith, 2009), bathymetry (Amante and Eakins, 2009), sediment thickness (Laske and Masters, 1997) and ocean isochron data (Müller et al., 2008). A continental breakup

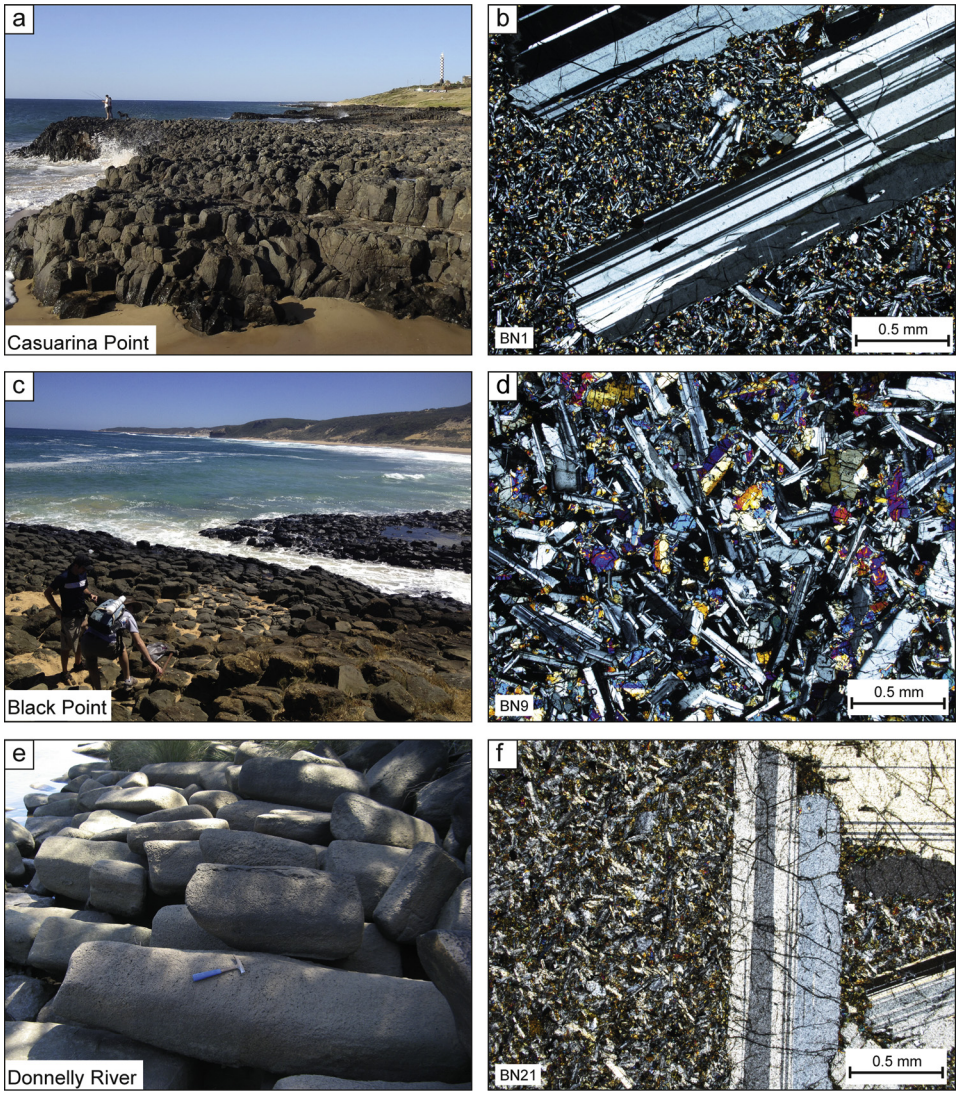

Fig. 2. Photographs (a, c, e) and photomicrographs (b, d, f) of selected samples that show petrography and freshness: (a–b) Cape Casuarina colonnade; (c–d) Black Point (Cape Gosselin) colonnade, and; (e–f) Donnelly River toppled colonnade.

age of 130 Ma has been used to define the cooling age of continental margin lithosphere, appropriate to the Perth Basin margin. Example applications elsewhere of the gravity methodology, with discussion of input parameter sensitivities, are given in Torsvik et al. (2015).

5. Results

5.1. $^{40}Ar/^{39}Ar$ results of the Bunbury Basalt

Three low-precision plateau ages were obtained from the three samples analyzed on the MAP215-50 (Table 2). Sample BN 6 from the Gelorup quarry yielded a plateau age of 136.5 ± 4.5 Ma (MSWD = 0.67, $P = 0.74$). Samples BN 10 and BN 12 from Black Point yielded plateau ages of 144 ± 9 Ma (MSWD = 0.35, $P = 0.98$) and 133 ± 8 Ma (MSWD = 0.33, $P = 0.95$), respectively. The samples from Black Point are part of the same flow and should therefore be the same age. The very high uncertainties associated with these ages are a result of low K/Ca ratios in plagioclase from the Bunbury Basalt, mostly ranging between 0.002 and 0.008 (equivalent to Ca/K = 125–500). Aliquots of BN 10 and 12 (BN 10-A and BN 12-A) were run on the ARGUS VI to determine whether a multi-collection instrument yielded more precise ages. Samples BN 10-A and BN 12-A yielded ages of 130.6 ± 1.0 Ma (MSWD = 1.32, $P = 0.16$) and 130.3 ± 1.3 Ma (MSWD = 0.67, $P = 0.87$), respectively, concordant within error, and as expected for a single flow from Black Point. The ARGUS VI yielded ages 5–10 times more precise than the MAP 215-50 for exceptionally low K/Ca samples like the Bunbury Basalt. The remaining Bunbury Basalt samples were therefore run on the ARGUS VI.

In total, nine high-precision plateau ages were obtained from the ten samples analyzed on the ARGUS VI (Fig. 3, Table 2). These nine ages define three distinct populations. The oldest age cluster from Donnelly River and sample BN4 from the Gelorup quarry have ages between 137.63 ± 0.89 and 136.50 ± 0.87 (MSWD = 0.62–1.52; $P = 0.12$–0.88). The second oldest cluster of ages from Casuarina Point and sample BN 3 from the Gelorup quarry have ages between 133.43 ± 0.75 and 132.17 ± 0.89 Ma (MSWD = 0.82–1.62; $P = 0.08$–0.45). The youngest ages are recorded at Black Point at 130.6 ± 1.0 and 130.3 ± 1.3 (MSWD = 0.67–1.32; $P = 0.16$–0.87).

One sample, BN 24, did not yield a plateau (see supplementary data tables). This sample probably absorbed excess argon from crustal contamination.

Table 2
Summary of plateau and inverse isochrons ages for concordant $^{40}Ar/^{39}Ar$ lava flow analyses.

General characteristics			Plateau characteristics				Isochron characteristics					
Sample no	K/Ca	Machine	Plateau age (Ma $\pm 2\sigma$)	Total ^{39}Ar released (%)	MSWD	P	Inv. isochron age (Ma $\pm 2\sigma$)	n	$^{40}Ar/^{36}Ar$ intercept ($\pm 2\sigma$)	MSWD	P	Spreading factor (%)
Casuarina Point												
BN 1	0.0058	ARGUS VI	132.17 ± 0.89	82	1.50	0.13	133.0 ± 4.2	14	277 ± 93	1.62	0.08	27
BN 2	0.0059	ARGUS VI	133.43 ± 0.75	95	1.30	0.16	134.1 ± 2.2	19	287 ± 44	1.38	0.13	23
Gelorup Quarry												
BN 3	0.0075	ARGUS VI	132.45 ± 0.65	92	1.00	0.45	133.4 ± 1.2	16	272 ± 29	0.82	0.65	65
BN 4	0.0077	ARGUS VI	136.90 ± 0.84	78	1.43	0.14	137.6 ± 2.9	13	269 ± 99	1.52	0.12	19
BN 6	0.0075	MAP 215-50	136.5 ± 4.5	96	0.67	0.74	137 ± 6	10	295 ± 16	0.73	0.66	48
Black Point (Cape Gosselin)												
BN 10	0.0021	MAP 215-50	144 ± 9	96	0.35	0.98	139 ± 17	13	312 ± 42	0.34	0.98	55
BN 10-A	0.0042	ARGUS VI	130.6 ± 1.0	93	1.32	0.16	134 ± 6	20	236 ± 71	1.27	0.20	21
BN 12	0.0029	MAP 215-50	133 ± 8	80	0.33	0.95	132 ± 12	9	300 ± 33	0.38	0.92	48
BN 12-A	0.0034	ARGUS VI	130.3 ± 1.3	86	0.67	0.87	128.1 ± 3.1	21	338 ± 49	0.57	0.93	33
Donnelly River												
BN 21	0.0059	ARGUS VI	136.85 ± 0.88	100	0.95	0.52	136.71 ± 0.91	19	300 ± 2.5	0.91	0.57	79
BN 22	0.0060	ARGUS VI	136.50 ± 0.87	100	0.58	0.91	136.47 ± 0.91	19	299 ± 4.3	0.62	0.88	71
BN 23	0.0059	ARGUS VI	137.63 ± 0.89	88	0.75	0.75	137.6 ± 1.0	17	301 ± 17	0.79	0.69	38

[a] Mean Square of Weighted Deviates (MSWD) and probability of fit (P) for plateau and isochron, percentage of ^{39}Ar degassed used in the plateau calculation, number of analyses included in the isochron, and $^{40}Ar/^{36}Ar$ intercept are indicated. Analytical uncertainties on the ages are quoted at 2 sigma (2σ) confidence levels.

5.2. Major and trace element geochemistry

All the volcanic samples are fresh with a loss on ignition (LOI) lower than 1 wt% (see online supplementary material). They plot as basalts or basaltic andesites in the total alkalis *vs.* silica (TAS) diagram in the subalkaline domain (Fig. 4), and can therefore be classified as continental tholeiitic basalts. All samples are slightly evolved as shown by their MgO content (5–6 wt%).

The Bunbury Basalt samples show incompatible and rare earth elements (REE) patterns similar to average enriched MORBs (Fig. 4, see supplementary material for full table). Specifically, the samples display slight enrichment in the most incompatible elements such as large ion lithophile elements (LILE; e.g., Rb, Cs, Ba) and light REE ($La_{CN}/Sm_{CN} = 0.89–1.74$; CN: ratio normalized to chondrite values from Sun and McDonough, 1989). The samples have flat patterns from moderate to least incompatible elements ($Dy_{CN}/Yb_{CN} = 1.06–1.56$). The samples also show positive Pb and negative Nb anomalies indicative of a contribution of continental lithosphere in the chemical characteristics of the basalts. Such characteristics are common to many continental flood basalts, such as Karoo (e.g., Jourdan et al., 2007) and the Central Atlantic Magmatic Province (e.g., Merle et al., 2014). Gosselin-type basalts are slightly more enriched in light REE ($La_{CN}/Sm_{CN} = 1.43–1.74$) and have flatter heavy REE patterns ($Dy_{CN}/Yb_{CN} = 1.06–1.26$) than Casuarina-type basalts ($La_{CN}/Sm_{CN} = 1.11–1.40$; $Dy_{CN}/Yb_{CN} = 1.28–1.56$).

On a Th/Yb *vs.* Nb/Yb discrimination diagram (Fig. 4d), the Bunbury Basalt displays mantle-like values ranging between N- and E-MORB similar to the Kerguelen Plateau to higher Th/Yb ratios that may be associated with a contribution from the continental lithosphere. In particular, the Casuarina-type basalts show a trend from mantle-like ratios towards higher Th/Yb for little variation in Nb/Yb ratios, which indicates a variable contribution from the continental crust (Fig. 4d). Such a trend is also shown by the Rajmahal traps (Ingle et al., 2004). The Gosselin-type basalts and the deep intrusive rocks plot away from the mantle array and have higher Th/Yb for the same Nb/Yb ratios as the Casuarina-type basalts indicating a stronger contribution from the continental crust (Fig. 4d).

5.3. Crustal basement thickness

The crustal basement thickness map (Fig. 5a) shows a thin oceanic crust within the Perth Abyssal Plain and a relatively sharp ocean–continent transition onto thick continental crust of the Yilgarn Craton to the north of the Bunbury Basalt. Further south, the E–W transition from thick cratonic crust to thin oceanic crust is much wider with a broad region of intermediate crustal thickness encompassing the Naturaliste Plateau, the Mentelle Basin and southern Perth Basin. The crust in the Mentelle Basin, in particular, is relatively extended ($\beta \approx 3$), but the Naturaliste Plateau and southern Perth are still relatively unstretched ($\beta \approx 1.4–1.6$). The superimposed shaded relief free-air gravity anomaly onto crustal thickness highlights the complex tectonic pattern of transform faults and abandoned sea-floor spreading axes that formed during the breakup of Australia from Greater India.

The Bunbury Basalt is predominantly situated on top of relatively thick crust (30–40 km; Fig. 5a) except in the northern portion where the crust is significantly thinner (~25 km). This NW–SE trending structure, known as the Harvey Ridge, is known to have a thinned sedimentary basin thickness and a relatively shallow depth to basement, which probably was a structural high from the end Permian onwards (Olierook and Timms, in press; Olierook et al., 2015c). Other thinner (~25 km) areas of continental basement thickness are poorly sampled (e.g., Naturaliste Plateau and Mentelle Basin) or distal to the relict breakup nexus (e.g, Houtman and Zeewyck sub-basins).

6. Discussion

6.1. Discussion of previously published ages and new $^{40}Ar/^{39}Ar$ plagioclase ages

Prior to this study, the Bunbury Basalt had been characterized by seven $^{40}Ar/^{39}Ar$ ages for five whole rock samples and two aliquots from one plagioclase separate (see online supplementary material) (Coffin et al., 2002; Frey et al., 1996; Pringle et al., 1994). Whole-rock $^{40}Ar/^{39}Ar$ analyses of basalt older than Cenozoic, which notoriously contain cryptic alteration, might yield apparent plateau ages that significantly depart from the true emplacement age (Verati and Jourdan, 2014). Of the previous analyses, only the plagioclase separates from Casuarina Point yielded a reliable plateau age at *ca.* 132 Ma (Coffin et al., 2002). This age should be recalculated using the constants and standard ages of Renne et al. (2011) or at least it should be calibrated against a set of constants. However, the standard used to measure this age is not calibrated against any internal standard, which precludes recalculation of the age of the sample and making it difficult to compare to our results. Since a sample from the same flow has been re-dated in the present study, we choose to use our new dataset of results,

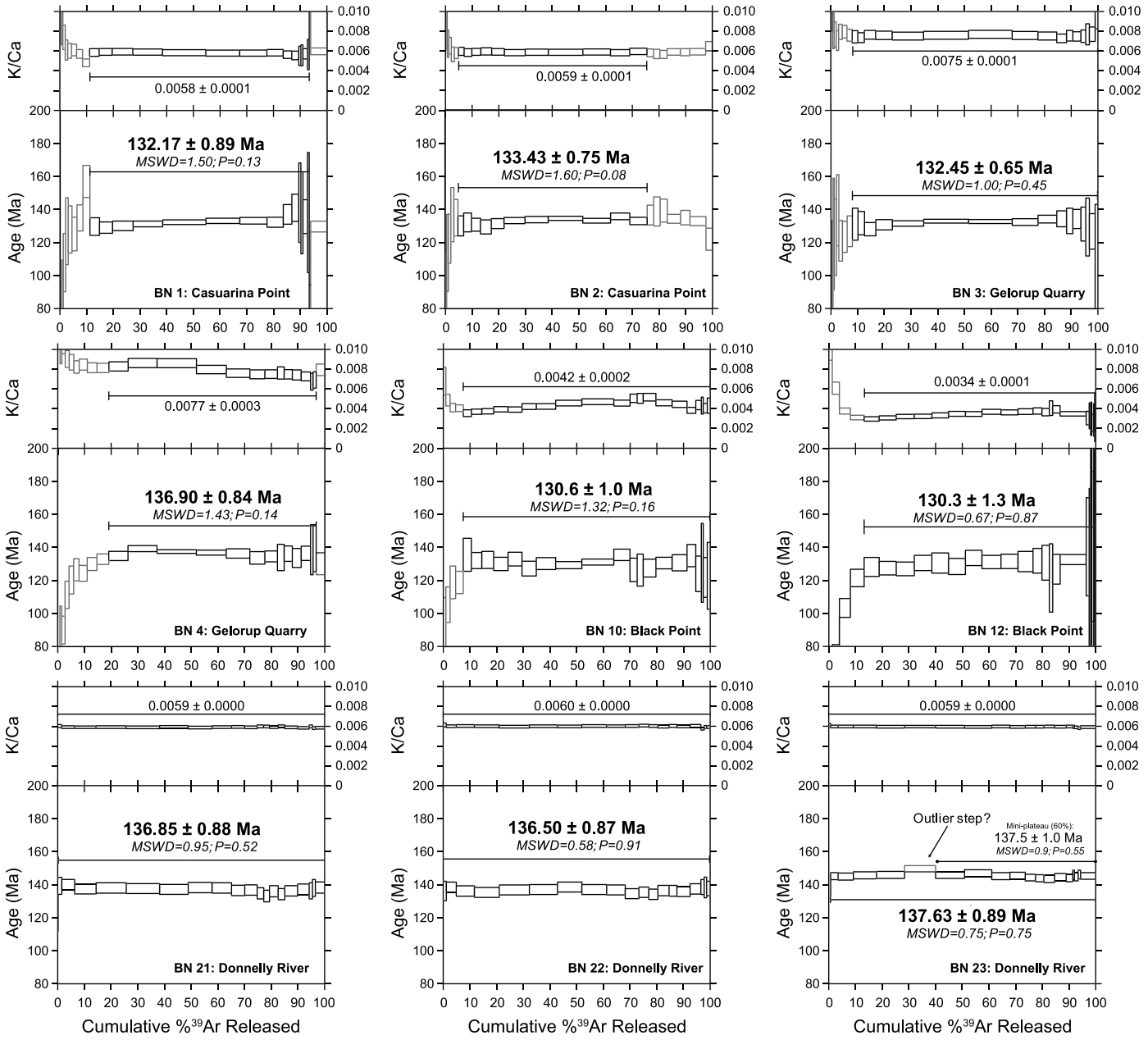

Fig. 3. $^{40}Ar/^{39}Ar$ apparent age and related K/Ca ratio spectra of the plagioclase separates versus the cumulative percentage of ^{39}Ar released measured on the ARGUS VI that yielded concordant plateau ages. Errors on plateau ages are quoted at 2σ. Ages in bold represent the most reliable ages for each sample. See online supplementary material for full analytical details.

based on the $^{40}Ar/^{39}Ar$ dating that we carried out using the latest generation of multi-collection instrumentation.

From our thirteen analyses, only nine samples yielded robust and high-precision plateau ages. These ages fall into three distinct age clusters. As each group is associated with what we interpret as a single flow, a weighted mean age for each group has been calculated (Fig. 6). The oldest cluster of four samples from Donnelly River and sample BN 4 from the Gelorup quarry yielded a mean age at 136.96 ± 0.43 Ma ($P = 0.32$). We suspect sample BN 4 was collected from blasted rocks belonging to the lower flow of Bunbury Paleovalley. The Donnelly River samples also represent the lower flow (Olierook et al., 2015b). The Bunbury Basalt at the Donnelly River and Gelorup quarry sites has not previously been dated. An age population at *ca.* 137 Ma is the oldest ever dated from the Bunbury Basalt.

The second cluster of three samples from Casuarina Point and sample BN 3 from the Gelorup Quarry has a mean age of 132.71 ± 0.43 Ma ($P = 0.06$; Fig. 6). Based on these data, we suspect that BN 3 was sampled from blasted rock from the upper flow of the Bunbury Paleovalley. The upper flow is the same as the outcrops at Casuarina Point (Olierook et al., 2015b).

The youngest cluster of two samples from Black Point yields a mean age of 130.45 ± 0.82 Ma ($P = 0.68$; Fig. 6). Olierook et al. (2015b) suggested that Black Point may be part of the same flow as Casuarina Point, although recognizing that previous workers noted geochemical discrepancy between the two localities (Frey et al., 1996; Ingle et al., 2004, 2002). The new age of *ca.* 130.5 Ma implies that Black Point is in fact a distinct flow younger than that from Casuarina Point. Its stratigraphic and geographic relationship to the other flows remains uncertain.

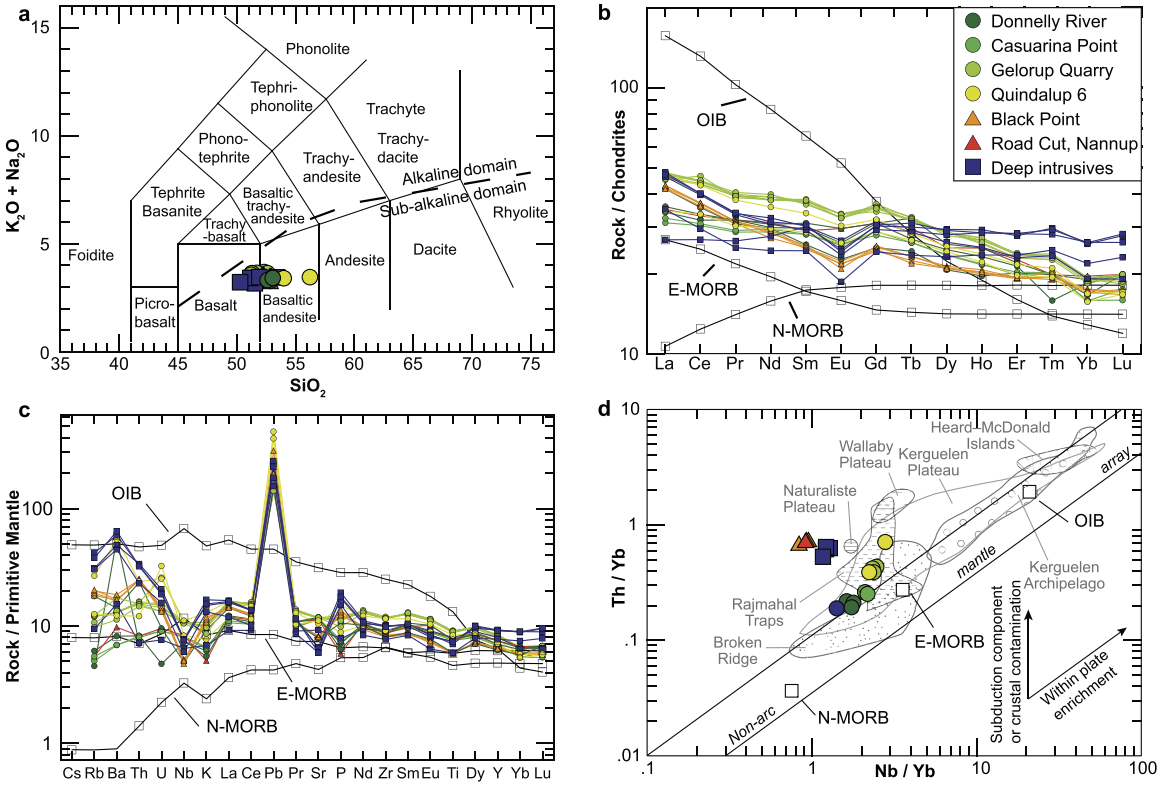

Fig. 4. Geochemistry discrimination diagrams for the Bunbury Basalt. (a) Total alkalis *vs.* silica (TAS) diagram with alkaline/sub-alkaline line from Miyashiro (1974). (b) Rare-earth element (REE) diagram normalized to CI chondrite. (c) Incompatible element (IE) plot normalized to primitive mantle. (d) Nb/Yb versus Th/Yb, after Shervais (1982). See online supplementary material for geochemistry data for shaded fields and respective sources. Normalization, normal mid-ocean ridge basalts (N-MORB), enriched MORB (E-MORB) and ocean island basalt (OIB) values from Sun and McDonough (1989). Bunbury Basalt points: circles = Casuarina-type; triangles = Gosselin-type; squares = Whicher-type.

No samples from the Donnelly Paleovalley yielded any plateau ages, so the age(s) of these flows remains unknown.

6.2. Causes and mechanisms for the emplacement of the Bunbury Basalt

The earliest recorded eruption of the Bunbury Basalt and the initial breakup of Gondwana, as indicated from plate reconstructions, both occurred at *ca.* 137–136 Ma (Gibbons et al., 2012) (Fig. 5). This synchronicity suggests a common cause, which remains to be identified. Is it possible that the Bunbury Basalt erupted as a result of decompression melting due to plate stretching, or was some form of geochemical enrichment or a higher geotherm required? Was the Bunbury Basalt's eruption driven by the proto-Kerguelen mantle plume, either as melt or heat source, as has previously been suggested (Coffin et al., 2002; Frey et al., 1996; Ingle et al., 2002)?

6.2.1. Plume-related models

Ingle et al. (2004) have shown, *via* Hf and Os isotope initial ratios, that the Casuarina-type basalts cannot be explained by mixing of an asthenosphere-like depleted upper mantle source with subcontinental lithospheric mantle (SCLM), instead suggesting that the involvement of an enriched deep mantle source was necessary. If the Kerguelen plume was, at least partially, responsible for the Bunbury Basalt, then the plume must have been incubating underneath the Gondwanan lithosphere at 137 Ma (Fig. 5, Fig. 7). Although it has been suggested that a plume was resident underneath Antarctica as far back as the Jurassic–Cretaceous boundary at *ca.* 145 Ma (Zhu et al., 2009), the position of the plume head has only been modeled from 131 Ma onwards (Antretter et al., 2002). Given that apparent polar wander paths indicate no evidence for global plate re-organizations from 105 to 200 Ma (Matthews et al., 2012), it is justified to infer that the relative motion of the plate above a quasi-stationary plume head (Koppers et al., 2012) was in the same direction relative to the Australian–Antarctic plate since 140 Ma. Using recent plate reconstructions (Gibbons et al., 2012), we project the position of the plume head back to 140 Ma in a relative ESE direction (Fig. 5). At 137 Ma, the center of the plume head is below the proto-Antarctic continent, ~700 km south of the eruptive center(s) of the Bunbury Basalt and ~500 km from the nascent mid-ocean spreading center (Fig. 5). The relatively small distance between the eruptive centers and the position of the plume head permits a plume origin for the Bunbury Basalt taking into account uncertainties associated with a quasi-stationary plume.

Comparatively small volumes of lava, such as the 90 km^3 of Bunbury Basalt, that are precursor to a main magmatic pulse are common in the geologic record but are not ubiquitous. The volcano-tectonic events surrounding the birth of the Iceland plume and plate dispersal in the North Atlantic are associated with early, tholeiitic lavas over a large area (western Greenland, eastern Greenland, Faroe Islands and NW Britain) with the plume center beneath eastern Greenland – all around 61–60 Ma (Torsvik et al., 2015). These lavas represent rather small volumes compared with the main pulse of magma that erupted at 56–55 Ma. On the contrary, geochronological constraints from the Karoo, Central Atlantic Magmatic Province and Paraná-Etendeka continental flood basalt provinces show that there the main pulse of magmatic activity is a continuous phase that also yields tholeiitic basalts (Jourdan et al., 2008; Nomade et al., 2007). These examples are not associated with precursor, tholeiitic volcanism.

It is perhaps peculiar that there is no evidence for other precursor volcanic events geographically in between the Bunbury Basalt and the proto-Kerguelen plume head. That being said, there are

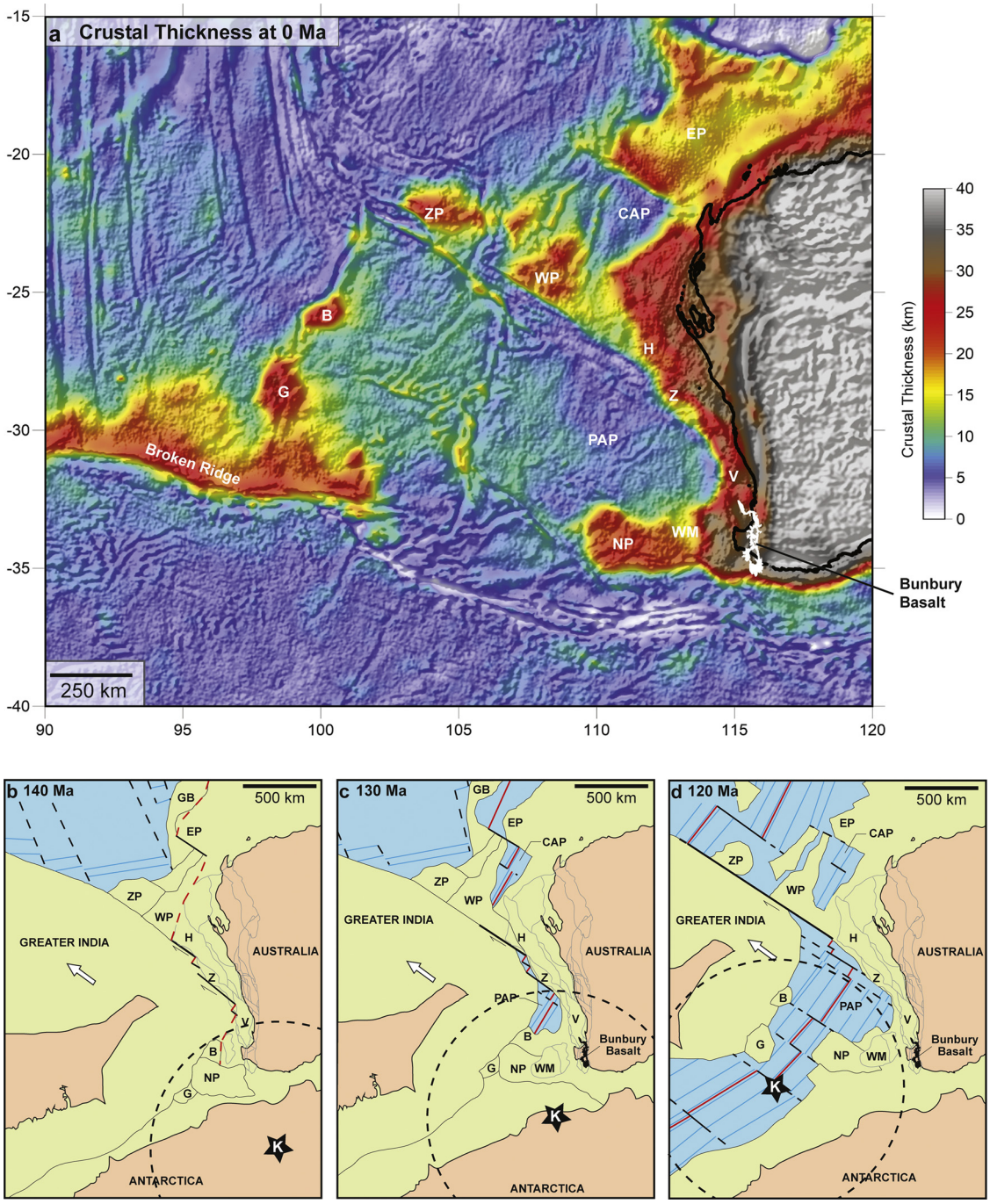

Fig. 5. (a) Present day crustal basement thickness determined from gravity inversion with superimposed shaded relief free-air gravity anomaly. (b–d) Plate reconstructions before, during and after the breakup of Greater India from the Austral–Antarctic portion of Gondwana, modified from Gibbons et al. (2012): (a) 140 Ma; (b) 130 Ma; (c) 120 Ma. B = Batavia Knoll; CAP = Cuvier Abyssal Plain; EP = Exmouth Plateau; FZ = Fracture Zone; G = Gulden Draak Knoll; GB = Gascoyne Block; H = Houtman Sub-Basin; NP = Naturaliste Plateau; PAP = Perth Abyssal Plain; V = Vlaming Sub-Basin; WM = Western Mentelle Basin; WP = Wallaby Plateau; Z = Zeewick Sub-basin; ZP = Zenith Plateau. K = center of Kerguelen mantle plume head, using reconstruction parameters from Antretter et al. (2002) and shown with 2000 km diameter plume head.

still several un- and under-explored regions situated between the Bunbury Basalt and the calculated Kerguelen plume position at 137–130 Ma that could have plume-derived volcanism present. Based on recent seismic work by Geoscience Australia (Borissova et al., 2010), the Naturaliste Plateau and western Mentelle Basin have significant potential to contain precursor volcanic rocks. The Mentelle Basin, in particular, given its significantly extended nature ($\beta \approx 3$, Fig. 5a), is a strong contender to contain plume-derived volcanics but the basin has yet to be drilled. If precursor volcanic rocks were found, this would provide a much more convincing piece of evidence that the Bunbury Basalt was indeed derived from the Kerguelen plume.

Coupled with the geochemical similarity between the Bunbury Basalt and Kerguelen plume-derived volcanic rocks, a deep mantle plume is a plausible explanation for the Bunbury Basalt.

6.2.2. *Models involving shallow mantle melting*

The new age constraints place the Bunbury Basalt coeval with the breakup along the western Australian margin, which implies that passive rifting may be an alternative explanation for the gen-

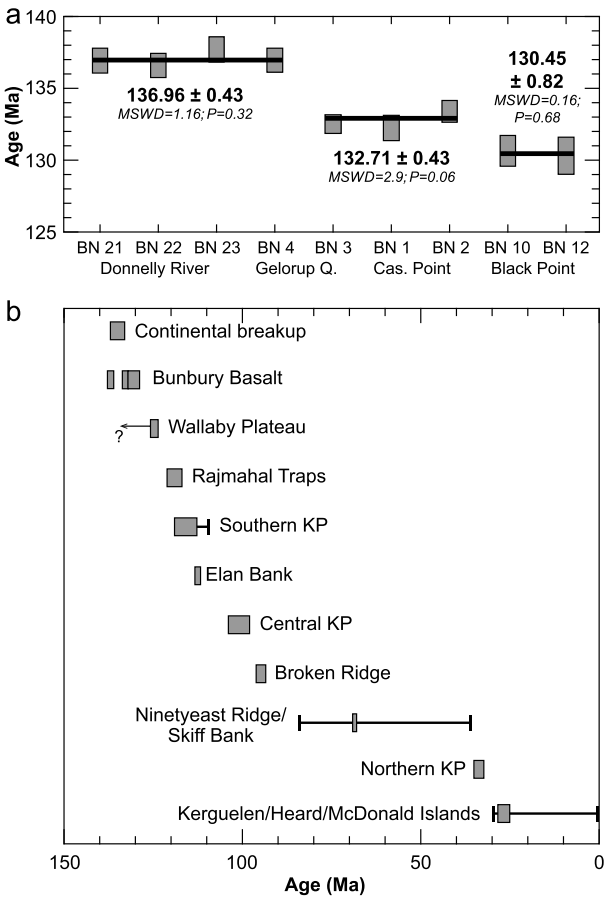

Fig. 6. (a) Weighted averages for three age clusters of the Bunbury Basalt (2σ internal errors). Q. = Quarry, Cas. = Casuarina. (b) Plagioclase $^{40}Ar/^{39}Ar$ plateau ages for volcanism postulated to be related to the Kerguelen mantle plume in grey boxes (Coffin et al., 2002; Duncan, 2002; Nicolaysen et al., 2000; Olierook et al., 2015a; Weis et al., 2002), whole-rock Ar/Ar plateau ages as black arrows (cf. Coffin et al., 2002) and the onset of breakup of Greater India and Australia based on earliest magnetic anomalies in the Perth Abyssal Plain (M10N or M10) (Gibbons et al., 2012).

esis of the Bunbury Basalt. The classic shallow mantle melting model involves the passive rise of the sub-lithospheric asthenosphere due to within-plate extensional strain (Foucher et al., 1982). In this model, the adiabatic rise of the asthenosphere is likely to produce melting via decompression. The crust below the Perth Basin is insufficiently stretched ($\beta \approx 1.4$) to permit decompression melting (Fig. 5a). A beta-factor of 3 is usually necessary unless additional heat is present or the geochemistry of the sublithospheric has been enriched (Chappell and Kusznir, 2008). The melting process can also be aided by fluids transferred via lithospheric faults active during rifting, thereby causing metasomatism of the subcontinental lithospheric mantle (SCLM). Metasomatised (hydrated) mantle requires a lower temperature and pressure to initiate melting than dry mantle (Kawamoto and Holloway, 1997). During the early stages of continental rifting, the produced melts are usually enriched liquids such as alkali basalts interpreted as derived from an enriched and metasomatised, subcontinental lithospheric mantle. As the rift evolves toward oceanization, moderately enriched melts similar to continental tholeiites or E-MORBs can be produced by the interaction of melts from the sub-lithospheric, depleted asthenosphere and the metasomatised SCLM. Note that the enriched and hydrated uppermost part of the asthenosphere, isolated from the convecting mantle under continents, may share chemical characteristics with the SCLM (Anderson, 1994). The interaction of depleted asthenosphere and SCLM is likely to produce a wide spectrum of basaltic liquids ranging in composition from N-MORBs to E-MORBs or continental tholeiites (Charpentier et al., 1998). Phases of MORB-like and alkaline magmatism could even alternate during the rifting process (Jagoutz et al., 2007). Such passive continental rifting is a possible explanation for the origin of the Bunbury Basalt in the context of eastern Gondwana breakup because it could account for the chemical composition of the Bunbury Basalt (Fig. 7).

Nevertheless, interaction between the ascending asthenosphere and the SCLM does not explain the geochemical similarities, including initial isotopic ratios, between the Kerguelen Plateau, the Rajmahal Traps, the Indian MORBs and the Bunbury Basalt. The geodynamical and chronological constraints suggest that not all of these magmatic activities were coeval or located close enough to be fed by the plume head (Fig. 5). The geochemical similarities suggest rather that a large domain of enriched mantle was sampled by these magmatic activities through time. Such a domain may be as large as the Dupal anomaly (Davies et al., 1989) and would lend more to a plume mechanism for mantle convection. Alternatively, it may be a more localized product from recycling of subducted oceanic lithosphere as has been shown elsewhere to yield similar geochemical signatures to those observed from the Bunbury Basalt (Hoernle et al., 2011). Such a recycled slab could exist under the relict NE India–SW Australia margin. The Pinjarra Orogen stretched at least 2000 km from north to south and sutured NE India to W Australia during the amalgamation of Gondwana at *ca.* 550–500 Ma (Fitzsimons, 2003). The oceanic crust that was subducted beneath Gondwana could have been tapped by both upwelling asthenosphere during rifting and, later, by the ascending Kerguelen mantle plume. Temperature differences between an ascending asthenosphere and mantle plume, together with contrasting space for magma ascent, could explain the differences in volumes for the Bunbury Basalt and the southern/central Kerguelen Plateau. A chemically-distinct SCLM source could also explain the enriched geochemical signature for the southern and central Kerguelen Plateau as opposed to those parts underlain by continental crust (Bénard et al., 2010). Alternatively, small heterogeneities, such as delaminated SCLM formed during continental rifting and later recycled into the passively upwelling shallow mantle during mid-ocean ridge spreading, could be scattered in the shallow mantle. Decompression melting of the SCLM heterogeneities in the distal part of the upwelling asthenosphere is likely to produce intraplate magmatism. Therefore, a plausible mechanism for the origin of the Bunbury Basalt involves melting an enriched patch of shallow mantle directly underneath the southern Perth Basin in the context of a much larger subducted SCLM (Fig. 7).

The breakup of Greater India and Australia is crucial in providing significant decompression melting of this enriched patch. Multiple rift events have been recorded that have thinned the continental crust in the southern Perth Basin during the Permian to Jurassic, but there is no evidence of Permian to Jurassic igneous rocks (Fig. 1b) (Olierook et al., 2015b, 2015c). Decompression melting could only be achieved when the crust was sufficiently thinned at the point of breakup during the Valanginian. The present-day crust is thinnest (~25 km) at the northern edge of the Bunbury Basalt (Fig. 5a). The Bunbury Basalt likely erupted at or near this portion of thinner crust (Olierook et al., 2015b). As the western Australian margin has been relatively quiescent since breakup (Olierook and Timms, in press), the present-day onshore crustal thickness is a good approximation for the thickness of the crust at the time of breakup. Crustal thickness has been shown elsewhere to be a factor in vertical magma ascent (Davies et al., 2015). Therefore, it is likely that the Bunbury Basalt erupted only in the southern Perth Basin because this was the only location where the crust was sufficiently thinned. Other ar-

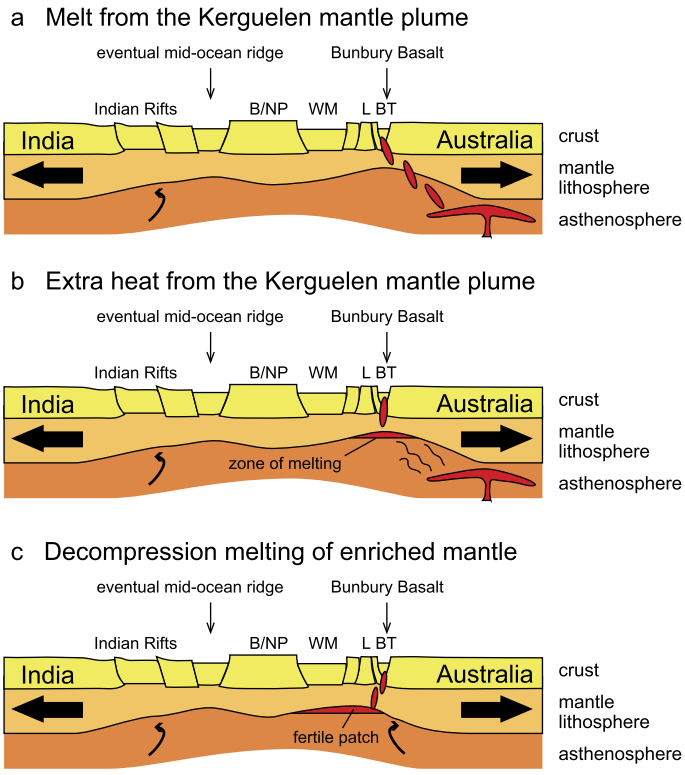

Fig. 7. Different cross-sectional models for the petrogenesis of the Bunbury Basalt and associated breakup of Greater India and Australia–Antarctica. (a) Melt generated from the Kerguelen mantle plume channeled to the Bunbury Trough. (b) Distal thermal perturbations from the Kerguelen mantle interacting with an already thinned and stretched lithosphere. The mantle plume provided an extra heat source necessary for the initiation of melting. (c) Decompression melting of an enriched, metasomatised shallow mantle. B = Batavia Knoll; NP = Naturaliste Plateau; WM = Western Mentelle Basin; L = Leeuwin Complex; BT = Bunbury Trough.

eas of significantly thin crust are either poorly sampled, distal to the postulated enriched patch of shallow mantle or were affected by significantly younger magmatic events (Olierook et al., 2015a; Pyle et al., 1995). Onshore, the basement adjacent to the Bunbury Basalt is significantly thicker (>30 km) (Fig. 5a). In these thick crustal regions, we suggest that magma underplated rather than ascended to the surface. The most likely mechanism for vertical ascent of the Bunbury Basalt is via intersections between the lithospheric-scale Darling Fault and subordinate deep-seated NW and NE-trending faults (Olierook et al., 2015b). There is a strong strike similarity of NE–SW sea floor spreading centers (Fig. 5), the NW–SE transforms in the proto-Perth Abyssal Plain and the faults in the Perth Basin (Olierook et al., 2015c). Therefore, it can be reasonably assumed that structural discontinuities were active simultaneously during continental breakup and so have acted as conduits for magma ascent.

7. Conclusions

1. New high-precision geochronology of the Bunbury Basalt in southwestern Australia has yielded three weighted mean ages of 136.96 ± 0.43 Ma, 132.71 ± 0.43 Ma and 130.45 ± 0.82 Ma, implying at least three pulses of magmatism in the southern Perth Basin, spread over a period of 7 m.y.
2. Recognized Kerguelen plume products and the Bunbury Basalt share geochemical similarities. Coupled with a distance of only 500–700 km between the plume head and the eruptive centers, a mantle plume is a distinct possibility for the genesis of the Bunbury Basalt.
3. The oldest Bunbury Basalt ages are synchronous with the breakup of eastern Gondwana and the initial opening of the Indian Ocean at *ca.* 137–136 Ma suggesting that a breakup-related cause may be an alternative. Since the crust is insufficiently thinned in onshore southwestern Australia, a geochemical enrichment was necessary to generate decompression melting. We propose that the Bunbury Basalt could have been produced from a patch of enriched shallow mantle beneath the southern Perth Basin by decompression melting related to passive rifting between Greater India and Australia and was able to ascend to the surface through relatively thin (~25 km) continental crust.

Acknowledgements

The authors would like to thank the following: the Geological Survey of WA for their access to core and drill cuttings; the Department of Water for their borehole logs; the Department of Environment & Conservation, the City of Bunbury and Holcim for their permission to sample outcrops; GEOROC for their geochemistry compilation database; C. Mayers and R.A. Frew in the WA Argon lab for help in sample preparation and analysis. F. Corfu and an anonymous reviewer are thanked for their constructive reviews that greatly improved the manuscript.

Appendix A. Supplementary material

Supplementary material related to this article can be found online at http://dx.doi.org/10.1016/j.epsl.2016.02.008.

References

Alvey, A., Gaina, C., Kusznir, N.J., Torsvik, T.H., 2008. Integrated crustal thickness mapping and plate reconstructions for the high Arctic. Earth Planet. Sci. Lett. 274, 310–321.

Amante, C., Eakins, B.W., 2009. ETOPO1 1 arc-minute global relief model: procedures, data sources and analysis. NOAA Technical Memorandum NESDIS NGDC-24. National Geophysical Data Center, NOAA [24 June 2014].

Anderson, D.L., 1994. The sublithospheric mantle as the source of continental flood basalts; the case against the continental lithosphere and plume head reservoirs. Earth Planet. Sci. Lett. 123, 269–280.

Antretter, M., Steinberger, B., Heider, F., Soffel, H., 2002. Paleolatitudes of the Kerguelen hotspot: new paleomagnetic results and dynamic modeling. Earth Planet. Sci. Lett. 203, 635–650.

Backhouse, J., 1988. Palynology of Cowaramup Line 7A: Western Australia. Geological Survey of Western Australia, Perth. Retrieved from http://geodocs.dmp.wa.gov.au/.

Bénard, F., Callot, J.-P., Vially, R., Schmitz, J., Roest, W., Patriat, M., Loubrieu, B., 2010. The Kerguelen plateau: records from a long-living/composite microcontinent. Mar. Pet. Geol. 27, 633–649.

Borissova, I., Bradshaw, B.E., Nicholson, C.J., Payne, D.S., Struckmeyer, H.I.M., 2010. New exploration opportunities on the southwest Australian margin – deep-water frontier Mentelle Basin. APPEA J. 50, 1–13.

Borissova, I., Coffin, M.F., Charvis, P., Operto, S., 2003. Structure and development of a microcontinent: Elan Bank in the southern Indian Ocean. Geochem. Geophys. Geosyst. 4, 1071.

Borissova, I., Totterdell, J., Southby, C., Owen, K., Bernardel, G., 2015. Characteristics of the Frontier Northern Houtman sub-basin formed on a magma-rich segment of the western Australian margin. In: AAPG/SEG International Conference & Exhibition. Melbourne, Australia.

Chappell, A.R., Kusznir, N.J., 2008. Three-dimensional gravity inversion for Moho depth at rifted continental margins incorporating a lithosphere thermal gravity anomaly correction. Geophys. J. Int. 174, 1–13.

Charpentier, S., Kornprobst, J., Chazot, G., Cornen, G., Boillot, G., 1998. Lithosphere–asthenosphere interaction during continental breakup: preliminary isotopic data on the passive Galicia margin (North-Atlantic). C. R. Acad. Sci., Sér. 2a, Sci. Terre Planètes 376, 757–762.

Coffin, M.F., Pringle, M.S., Duncan, R.A., Gladczenko, T.P., Storey, M., Müller, R.D., Gahagan, L.A., 2002. Kerguelen hotspot magma output since 130 Ma. J. Petrol. 43, 1121–1139.

Davies, D.R., Rawlinson, N., Iaffaldano, G., Campbell, I.H., 2015. Lithospheric controls on magma composition along Earth's longest continental hotspot track. Nature 525, 511–514.

Davies, H.L., Sun, S.-S., Frey, F.A., Gautier, I., McCulloch, M.T., Price, R.C., Bassias, Y., Klootwijk, C.T., Leclaire, L., 1989. Basalt basement from the Kerguelen Plateau and trail of a Dupal plume. Contrib. Mineral. Petrol. 103, 457–469.

Duncan, R.A., 2002. A time frame for construction of the Kerguelen Plateau and broken ridge. J. Petrol. 43, 1109–1119.

Fitzsimons, I.C.W., 2003. Proterozoic basement provinces of southern and southwestern Australia, and their correlation with Antarctica. In: Yoshida, M., Windley, B.F., Dasgupta, S. (Eds.), Proterozoic East Gondwana: Supercontinent Assembly and Breakup. Geological Society, London. Special Publications. pp. 93–130.

Foucher, J.-P., Pichon, X.L., Sibuet, J.-C., Roberts, D.G., Chenet, P.-Y., Bally, A.W., Oxburgh, E.R., Kent, P., Dewey, J.F., Bott, M.H.P., Jackson, J.A., Osmaston, M.F., Turcotte, D.L., 1982. The Ocean–continent transition in the uniform lithospheric stretching model: role of partial melting in the mantle [and discussion]. Philos. Trans. R. Soc., Math. Phys. Eng. Sci. 305, 27–43.

Franke, D., 2013. Rifting, lithosphere breakup and volcanism: comparison of magma-poor and volcanic rifted margins. Mar. Pet. Geol. 43, 63–87.

Frey, F.A., McNaughton, N.J., Nelson, D.R., deLaeter, J.R., Duncan, R.A., 1996. Petrogenesis of the Bunbury Basalt, Western Australia: interaction between the Kerguelen plume and Gondwana lithosphere? Earth Planet. Sci. Lett. 144, 163–183.

Gibbons, A.D., Barckhausen, U., van den Bogaard, P., Hoernle, K., Werner, R., Whittaker, J.M., Müller, R.D., 2012. Constraining the Jurassic extent of Greater India: tectonic evolution of the West Australian margin. Geochem. Geophys. Geosyst. 13, Q05W13.

Hoernle, K., Hauff, F., Werner, R., van den Bogaard, P., Gibbons, A.D., Conrad, S., Muller, R.D., 2011. Origin of Indian Ocean Seamount province by shallow recycling of continental lithosphere. Nat. Geosci. 4, 883–887.

Ingle, S., Scoates, J.S., Weis, D., Brügmann, G., Kent, R.W., 2004. Origin of Cretaceous continental tholeiites in southwestern Australia and eastern India: insights from Hf and Os isotopes. Chem. Geol. 209, 83–106.

Ingle, S., Weis, D., Scoates, J.S., Frey, F.A., 2002. Relationship between the early Kerguelen plume and continental flood basalts of the paleo-Eastern Gondwanan margins. Earth Planet. Sci. Lett. 197, 35–50.

Jagoutz, O., Müntener, O., Manatschal, G., Rubatto, D., Péron-Pinvidic, G., Turrin, B.D., Villa, I.M., 2007. The rift-to-drift transition in the North Atlantic: a stuttering start of the MORB machine? Geology 35, 1087–1090.

Jones, A.T., Kelman, A.P., Kennard, J.M., Le Poidevin, S., Mantle, D.J., Mory, A.J., 2012. Offshore Perth Basin biozonation and stratigraphy 2011, chart 38. Geoscience Australia.

Jourdan, F., Féraud, G., Bertrand, H., Watkeys, M.K., 2007. From flood basalts to the inception of oceanization: example from the $^{40}Ar/^{39}Ar$ high-resolution picture of the Karoo large igneous province. Geochem. Geophys. Geosyst. 8, 02002.

Jourdan, F., Féraud, G., Bertrand, H., Watkeys, M.K., Renne, P.R., 2008. The $^{40}Ar/^{39}Ar$ ages of the sill complex of the Karoo large igneous province: implications for the Pliensbachian–Toarcian climate change. Geochem. Geophys. Geosyst. 9, Q06009.

Jourdan, F., Verati, C., Féraud, G., 2006. Intercalibration of the Hb3gr $^{40}Ar/^{39}Ar$ dating standard. Chem. Geol. 231, 177–189.

Kawamoto, T., Holloway, J.R., 1997. Melting temperature and partial melt chemistry of H_2O-saturated mantle peridotite to 11 gigapascals. Science 276, 240–243.

Klein, E.M., Langmuir, C.H., Staudigel, H., 1991. Geochemistry of basalts from the southeast Indian Ridge, 115°E–138°E. J. Geophys. Res., Solid Earth 96, 2089–2107.

Koppers, A.A.P., Yamazaki, T., Geldmacher, J., Gee, J.S., Pressling, N., Hoshi, H., Anderson, L., Beier, C., Buchs, D.M., Chen, L.H., Cohen, B.E., Deschamps, F., Dorais, M.J., Ebuna, D., Ehmann, S., Fitton, J.G., Fulton, P.M., Ganbat, E., Hamelin, C., Hanyu, T., Kalnins, L., Kell, J., Machida, S., Mahoney, J.J., Moriya, K., Nichols, A.R.L., Rausch, S., Sano, S.I., Sylvan, J.B., Williams, R., 2012. Limited latitudinal mantle plume motion for the Louisville hotspot. Nat. Geosci. 5, 911–917.

Laske, G., Masters, G., 1997. A global digital map of sediment thickness. Eos Trans. AGU 78, F483.

Matthews, K.J., Seton, M., Müller, R.D., 2012. A global-scale plate reorganization event at 105–100 Ma. Earth Planet. Sci. Lett. 355–356, 283–298.

Merle, R., Marzoli, A., Reisberg, L., Bertrand, H., Nemchin, A., Chiaradia, M., Callegaro, S., Jourdan, F., Bellieni, G., Kontak, D., Puffer, J., McHone, J.G., 2014. Sr, Nd, Pb and Os isotope systematics of CAMP tholeiites from Eastern North America (ENA): evidence of a subduction-enriched mantle source. J. Petrol. 55, 133–180.

Miyashiro, A., 1974. Volcanic rock series in island arcs and active continental margins. Am. J. Sci. 274, 321–355.

Müller, R.D., Sdrolias, M., Gaina, C., Steinberger, B., Heine, C., 2008. Long-term sea-level fluctuations driven by ocean basin dynamics. Science 319, 1357–1362.

Nicolaysen, K., Frey, F.A., Hodges, K., Weis, D., Giret, A., 2000. $^{40}Ar/^{39}Ar$ geochronology of flood basalts from the Kerguelen Archipelago, southern Indian Ocean: implications for Cenozoic eruption rates of the Kerguelen plume. Earth Planet. Sci. Lett. 174, 313–328.

Nomade, S., Knight, K.B., Beutel, E., Renne, P.R., Verati, C., Féraud, G., Marzoli, A., Youbi, N., Bertrand, H., 2007. Chronology of the Central Atlantic magmatic province: implications for the Central Atlantic rifting processes and the Triassic–Jurassic biotic crisis. Palaeogeogr. Palaeoclimatol. Palaeoecol. 244, 326–344.

Olierook, H.K.H., Merle, R.E., Jourdan, F., Sircombe, K., Fraser, G., Timms, N.E., Nelson, G., Dadd, K.A., Kellerson, L., Borissova, I., 2015a. Age and geochemistry of magmatism on the oceanic Wallaby Plateau and implications for the opening of the Indian Ocean. Geology 43, 971–974.

Olierook, H.K.H., Timms, N.E., in press. Quantifying multiple Permian–Cretaceous exhumation events during the breakup of eastern Gondwana: sonic transit time analysis of the central and southern Perth Basin. Basin Res. http://dx.doi.org/10.1111/bre.12133.

Olierook, H.K.H., Timms, N.E., Merle, R.E., Jourdan, F., Wilkes, P.G., 2015b. Paleodrainage and fault development in the southern Perth Basin, Western Australia during and after the breakup of Gondwana from 3D modelling of the Bunbury Basalt. Aust. J. Earth Sci. 62, 289–305.

Olierook, H.K.H., Timms, N.E., Wellmann, J.F., Corbel, S., Wilkes, P.G., 2015c. A 3D structural and stratigraphic model of the Perth Basin: implications for basin fill on the Western Australian margin during and after Gondwana. Aust. J. Earth Sci. 62, 447–467.

Pringle, M.S., Storey, M., Wijbrans, J., 1994. $^{40}Ar/^{39}Ar$ geochronology of mid-Cretaceous Indian Ocean basalts: constraints on the origin of large flood basalt provinces. Eos Trans. AGU 75, 728.

Pyle, D.G., Christe, D.M., Mahoney, J.J., Duncan, R.A., 1995. Geochemistry and geochronology of ancient southeast Indian Ocean and southwest Pacific Ocean seafloor. J. Geophys. Res. B, Solid Earth Planets 100, 22261–22282.

Renne, P.R., Balco, G., Ludwig, K.R., Mundil, R., Min, K., 2011. Response to the comment by W.H. Schwarz et al. on "Joint determination of ^{40}K decay constants and $^{40}Ar^*/^{40}K$ for the Fish Canyon sanidine standard, and improved accuracy for $^{40}Ar/^{39}Ar$ geochronology" by P.R. Renne et al. (2010). Geochim. Cosmochim. Acta 75, 5097–5100.

Renne, P.R., Swisher, C.C., Deino, A.L., Karner, D.B., Owens, T.L., DePaolo, D.J., 1998. Intercalibration of standards, absolute ages and uncertainties in $^{40}Ar/^{39}Ar$ dating. Chem. Geol. 145, 117–152.

Sandwell, D.T., Smith, W.H.F., 2009. Global marine gravity from retracked Geosat and ERS-1 altimetry: ridge segmentation versus spreading rate. J. Geophys. Res., Solid Earth 114, B01411.

Shervais, J.W., 1982. Ti–V plots and the petrogenesis of modern and ophiolitic lavas. Earth Planet. Sci. Lett. 59, 101–118.

Sun, S.-s., McDonough, W.F., 1989. Chemical and isotopic systematics of Oceanic Basalts: implications for mantle omposition and processes. Geol. Soc. (Lond.) Spec. Publ. 42, 313–345.

Torsvik, T.H., Amundsen, H.E.F., Trønnes, R.G., Doubrovine, P.V., Gaina, C., Kusznir, N.J., Steinberger, B., Corfu, F., Ashwal, L.D., Griffin, W.L., Werner, S.C., Jamtveit, B., 2015. Continental crust beneath southeast Iceland. Proc. Natl. Acad. Sci. USA 112, E1818–E1827.

van Wijk, J.W., Huismans, R.S., ter Voorde, M., Cloetingh, S., 2001. Melt generation at volcanic continental margins: no need for a mantle plume? Geophys. Res. Lett. 28, 3995–3998.

Verati, C., Jourdan, F., 2014. Modelling effect of sericitization of plagioclase on the $^{40}K/^{40}Ar$ and $^{40}K/^{39}Ar$ chronometers: implication for dating basaltic rocks and mineral deposits. Geol. Soc. (Lond.) Spec. Publ. 378, 155–174.

Weis, D., Frey, F.A., Schlich, R., Schaming, M., Montigny, R., Damasceno, D., Mattielli, N., Nicolaysen, K.E., Scoates, J.S., 2002. Trace of the Kerguelen mantle plume: evidence from seamounts between the Kerguelen Archipelago and Heard Island, Indian Ocean. Geochem. Geophys. Geosyst. 3, 1–27.

Whitmarsh, R.B., Manatschal, G., Minshull, T.A., 2001. Evolution of magma-poor continental margins from rifting to seafloor spreading. Nature 413, 150–154.

Williams, S.E., Whittaker, J.M., Granot, R., Müller, D.R., 2013. Early India–Australia spreading history revealed by newly detected Mesozoic magnetic anomalies in the Perth Abyssal Plain. J. Geophys. Res., Solid Earth 118, 3275–3284.

Williams, S.E., Whittaker, J.M., Müller, R.D., 2011. Full-fit, palinspastic reconstruction of the conjugate Australian–Antarctic margins. Tectonics 30, TC6012.

Zhu, D.-C., Chung, S.-L., Mo, X.-X., Zhao, Z.-D., Niu, Y., Song, B., Yang, Y.-H., 2009. The 132 Ma Comei-Bunbury large igneous province: remnants identified in present-day southeastern Tibet and southwestern Australia. Geology 37, 583–586.